Pressure measurements and high speed visualizations of the cavitation phenomena at deep part load condition in a Francis turbine

K Yamamoto[1], A Müller[1], A Favrel[1], C Landry[1], F Avellan[1]

[1]EPFL Laboratory for Hydraulic Machines, Av. de Cour 33bis, 1007 Lausanne, Switzerland

E-mail: keita.yamamoto@epfl.ch

Abstract. In a hydraulic power plant, it is essential to provide a reliable, sustainable and flexible energy supply. In recent years, in order to cover the variations of the renewable electricity production, hydraulic power plants are demanded to operate with more extended operating range. Under these off-design conditions, a hydraulic turbine is subject to cavitating swirl flow at the runner outlet. It is well-known that the helically/symmetrically shaped cavitation develops at the runner outlet in part load/full load condition, and it gives severe damage to the hydraulic systems under certain conditions. Although there have been many studies about partial and full load conditions, contributions reporting the deep part load condition are limited, and the cavitation behaviour at this condition is not yet understood. This study aims to unveil the cavitation phenomena at deep part load condition by high speed visualizations focusing on the draft tube cone as well as the runner blade channel, and pressure fluctuations associated with the phenomena were also investigated.

1. Introduction

In a hydraulic power plant, it is known that cavitation has undesirable effects on the systems. The first report about the phenomena called "power swing" observed in the hydraulic power plant was made by Rheingans [1]. He reported that the amplitude of pressure fluctuations can be magnified in certain conditions, and it gives a violent effect to the systems. After that, a number of surveys about cavitation phenomena observed in hydraulic power plants has been carried out in diverse ways. It was reported that the feature of cavitation has a strong dependence upon a discharge of an operating point as well as a turbine head. [2]

At full load operating condition of a Francis turbine, Jacob *et al.* primarily performed the experimental survey on the pressure surge, and they investigated the pressure fluctuations induced by this instability in 1990s [3]. Koutnik and Pulpitel applied the transfer matrix method to the full load condition for the purpose of stabilization analyses using the essential parameters of cavitation [4]. Recently, Müller *et al.* conducted a local flow and discharge analysis based on PIV measurements in the presence of a cavitating vortex rope for a better understanding of the self-excited pressure surge [5]. Alligné *et al.* carried out a parametric study of the draft tube flow to investigate the influence of various parameters on the unsteady cavitation phenomena with a one-dimensional model and they described the destabilizing effects of the flow swirl and the conical shape of the diffuser at full load condition [6].

At part load condition, the first study about the helical cavitation vortex rope in the elbow type draft tube was addressed by Nishi *et al.* [7]. They reported that there seems to be three different underlying spectral peaks of pressure oscillations in the cone, and the resonance occurs by the coincidence of the

frequency of pressure recovery variation governed by the vortex rope precession with the natural frequency of the draft tube system including the cavitation. This resonance was also reported by Favrel *et al*. They showed that the high amplitude of the pressure fluctuation is induced by the coincidence of the precession frequency with the natural frequency of the draft tube system [8].

Although a number of investigations into both full load and part load operating conditions is reported, the research about deep part load condition has not been well mentioned yet. To the author's knowledge, pressure measurements on the runner blade to investigate the fatigue life of the runner were conducted in the low discharge condition (about 30% of the nominal discharge) by Farhat and Lowys *et al*. [9] [10], however, they do not mention cavitation phenomena at this condition. In the present study, it is aimed at unveiling and investigating cavitation phenomena observed at deep part load condition by high speed visualizations and pressure fluctuation measurements.

2. Reduced scale model of a Francis turbine

2.1. Non-dimensional parameters of a reduced scale model of a Francis turbine

The sketch of a reduced scale model of a Francis turbine with essential components is shown in Fig. 1. In the reduced scale model, following non-dimensional parameters called flow rate factor Q_{ED} and speed factor n_{ED} are of key importance for the operation and performance of the turbine. These parameters are defined by the following equations.

$$Q_{ED} = \frac{Q}{D_{ref}^2 \sqrt{E}} \tag{1}$$

$$n_{ED} = \frac{n D_{ref}}{\sqrt{E}} \tag{2}$$

where Q represents the discharge, E the turbine specific energy, D_{ref} the turbine reference diameter, n the turbine rotational frequency (Hz). Thoma number which generally dictates the behaviour and development of the cavitation is defined by Net Positive Suction Energy (NPSE) as follows.
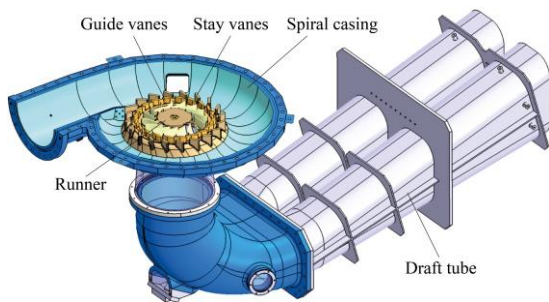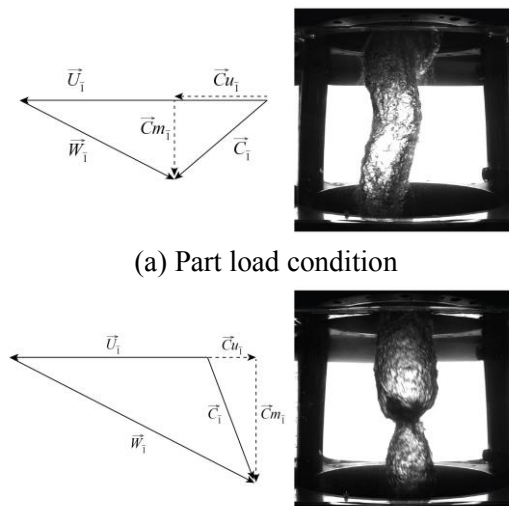
$$\sigma = \frac{NPSE}{E} \tag{3}$$

(a) Part load condition

Fig. 1 Sketch of a reduced scale model of a Francis turbine

(b) Full load condition

Fig. 2 Velocity triangles and shape of the cavitation vortex rope at each operating condition

2.2. Velocity triangle and cavitation vortex rope

At the best efficiency condition of the turbine (BEP), theoretically the flow leaves no swirling component at the runner outlet, meaning that the flow at the runner outlet is purely axial. However, the turbine is often requested to operate at an off-design condition. Under these conditions, the flow at the runner outlet is subject to a strong swirl velocity component. At part load condition ($Q < Q_{BEP}$), the flow is animated with a positive absolute circumferential velocity in the same sense as the runner revolution. At this condition, the helical shape vortex rope rolling up a central stalled region appears in the cone (see Fig. 2(a)). At full load condition ($Q > Q_{BEP}$), the peripheral velocity component of the flow leaving the runner is negative inducing the swirling flow rotating in the opposite direction of the runner rotation, and the flow forms the axisymmetric shape cavitation vortex rope at the centre of the cone (see Fig. 2(b)).

At deep part load condition, theoretically the peripheral velocity component becomes highly intense and the meridional component is very small, therefore the intense swirling flow and the large stagnation zone are formed at the runner outlet. Hence, the flow close to the runner becomes more important and cavitation may appear around the runner blade. In the present study, experiments were focused on the lower discharge than 40% of Q_{BEP}.

3. Experimental Setup

The entire experimental setup with a 1:16 reduced scale model of a Francis turbine is shown in Fig. 3. Totally 28 piezo-resistive pressure sensors were installed throughout the test rig, especially in the draft tube cone 8 sensors (4 sensors each at upper and lower sections) were installed. The torque acting on the shaft, mean discharge, turbine rotational frequency, and turbine specific energy were also monitored and recorded. The mean discharge was adjusted by the guide vane opening angle, and the turbine specific energy was controlled by the rotational frequency of two axial double-volute pumps. The pressure level in the draft tube was set by a vacuum pump in the downstream reservoir. At the best efficiency condition of this turbine (BEP), Q_{ED} and n_{ED} values are 0.20 and 0.288 respectively.
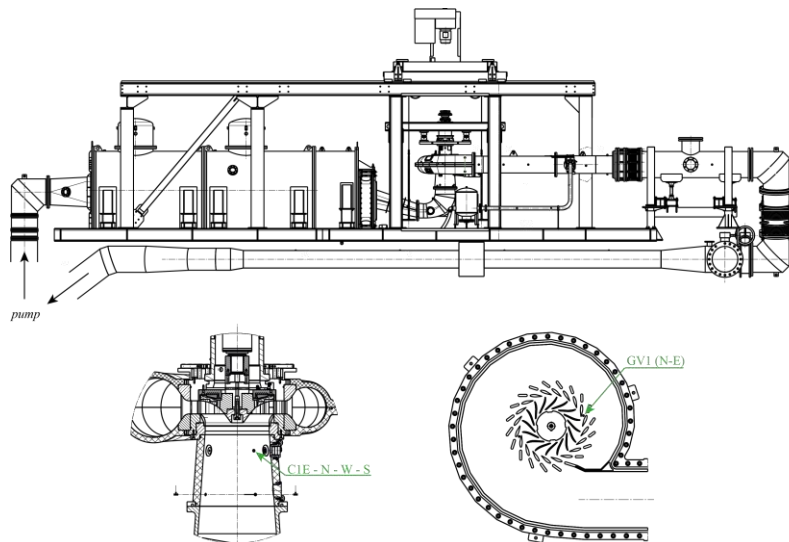

Fig. 3 Experimental configuration

In the experiment, two types of high-speed visualizations were carried out. The first one is for the cavitation vortex rope in the cone, and the second one is focused on the inter-blade cavitation vortices in the blade channel of the runner. Fig. 4 shows the experimental setup for each visualization and the cones used for these visualizations. These cones have respectively the rectangular and inclined windows filled with water to minimize the optical deformation. For the first visualization, the LED screen was used as a backlight source to have a better contrast between liquid and gaseous phases. For the second visualization, two types of lights, a stroboscope and an intense flash light, were prepared. The image of

both lights are shown in Fig. 5 and Fig. 6. The frequency of the strobe light emission was synchronized with the runner rotational frequency as well as the high speed image recording in order to capture the image of the same blade position at every one rotation of the runner (see Fig. 5(b)). The second intense light can generate a 11ms long intense flash permitting us to observe the cavitation behaviour in the blade channel with a high frame rate of the high speed camera such as 10,000 frames per second (see Fig. 6(b)). These two types of lights were used to capture the inter-blade cavitation vortices properly, and all the visualizations were synchronized with the pressure fluctuation measurement.
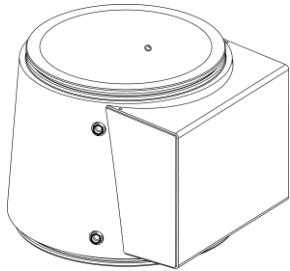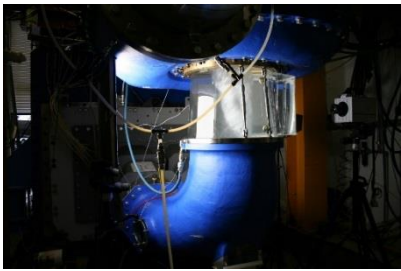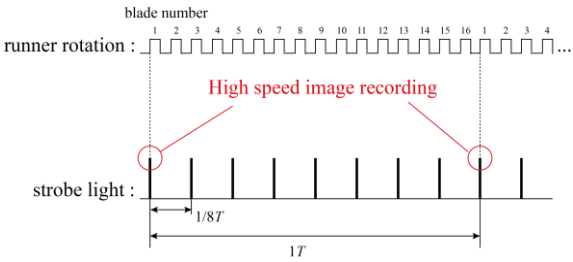

(a) Visualization setup for the cavitation vortex rope in the cone
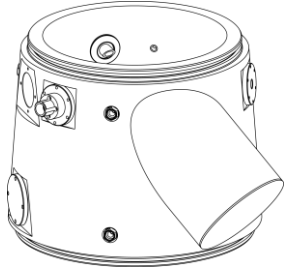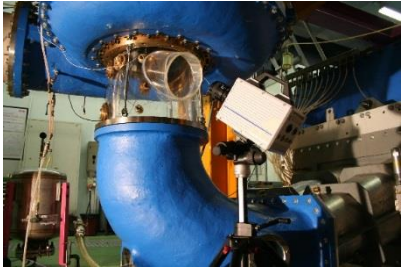
(b) Visualization setup for the inter-blade cavitation vortices in the blade channel
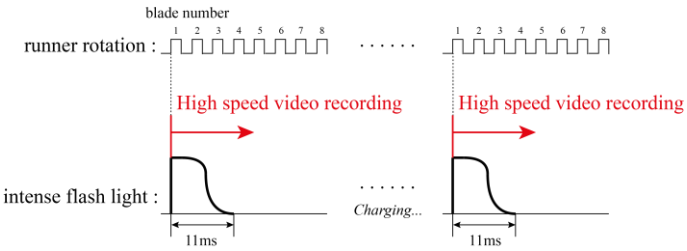
Fig. 4 Image of the visualization experimental setups

(a) Image of the strobe light (b) High speed image recording with the strobe light

Fig. 5 Image of the strobe light and high speed image recording


(a) Image of the intense flash light (b) High speed video recording with the intense flash light

Fig. 6 Image of the intense flash light and high speed video recording

4. Results

4.1. Vortex rope features

As mentioned above, it is well known that the helical shape cavitation vortex rope is observed at part load operating condition. This cavitation vortex rope is formed by a stalled region at the centre of the cone and the swirling flow rolling up this stalled region. The swirl intensity at the runner outlet becomes stronger as the decrease of discharge, which correspondingly causes the increase of the vortex rope precession frequency. In this section, the frequency and the behaviour of the cavitation vortex rope with several discharge values were investigated based on the frequency analysis (the one-sided autospectral density, Gxx) and the high speed visualization image. The frequency analysis results of one pressure sensor in the cone (at upper section, see Fig. 3) and images of cavitation vortex rope at $\sigma = 0.11$ and n_{ED} = 0.288 are shown in Fig. 7. In the part load condition (over 45% of Q_{BEP}), the shape of the cavitation vortex rope is well developed, correspondingly the spectral peak of the precession frequency is dominant (see Fig. 7 (b) and (c)). In the lower discharge than 45% to 30% of Q_{BEP}, although the cavitation vortex rope still remains, the shape of the rope becomes less obvious. In this discharge region, there seems to be two separated vortex ropes located in 180 degree positions in the cone, therefore the second spectral peak (almost double of the first peak) is more dominant than the first one in the frequency domain (see Fig. 7(c)). In the lower discharge than 30% of Q_{BEP}, the cavitation vortex rope is not observed any longer, and a huge stagnant region dominates the flow at the centre of the cone (see Fig. 7(e)), and there are almost no features of the pressure fluctuations in the draft tube cone. The visualizations for the blade channel to observe the inter blade cavitation vortices were mainly performed in this discharge condition, and the results are shown in the next section.
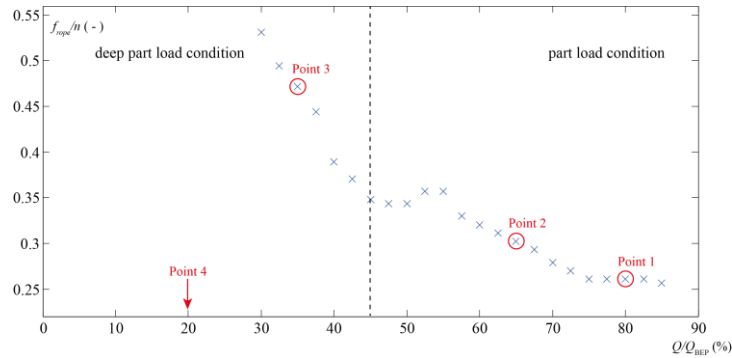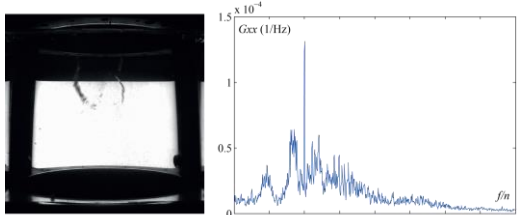

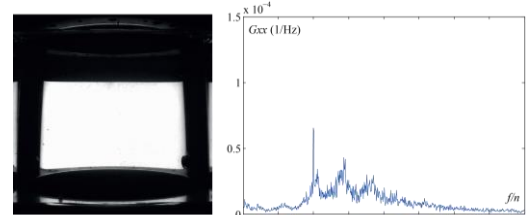(a) Non-dimensional frequency of the cavitaiton vortex rope presession
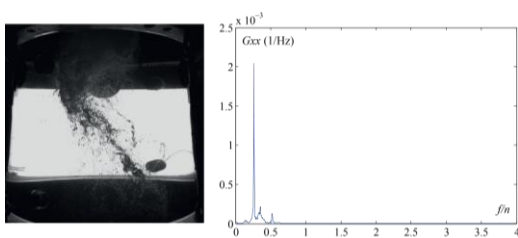
(b) Point 1, Q/Q_{BEP} = 0.80
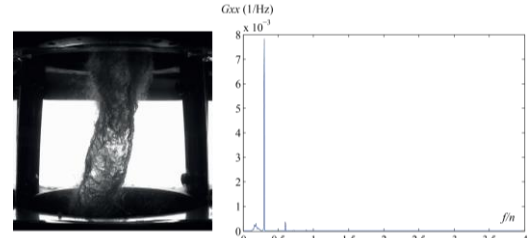
(c) Point 2, Q/Q_{BEP} = 0.65

(d) Point 3, Q/Q_{BEP} = 0.35

(e) Point 4, Q/Q_{BEP} = 0.20

Fig. 7 The cavitation vortex rope features at several operating points ($\sigma = 0.11$, n_{ED} = 0.288)

4.2. Inter-blade cavitation vortices

At discharge values lower than 30% of Q_{BEP}, the cavitation vortex rope in the cone disappears, thus the flow close to the runner becomes more and more important. It was reported that cavitation occasionally appears attaching on the runner blade, or inside the blade channel in the low discharge condition. [2] [11]. In the experiment, although there are no inter-blade cavitation vortices at the nominal n_{ED} value, the clear inter-blade cavitation vortices are observed at higher n_{ED} such as 110% of the nominal value and $Q_{ED} = 0.055$ (27.5% of Q_{BEP}) as shown in Fig. 8, which suggests that the incident angle of the flow at the turbine inlet was optimized. Key parameters of these operating points (i) and (ii) were summarized in Table 1. It seems that this vortices are formed by the flow separation in the blade channel, therefore the incident angle at the turbine inlet plays an important role on the onset of this vortex. The frequency analysis results of the pressure oscillations in the cone and guide vane (see Fig. 3) are shown in Fig. 9 and 10 respectively, however, the pressure fluctuation features in the frequency domain are similar in both cases. It should be noted that the effect of the inter-blade cavitation vortices is relatively minor at the presented condition and further investigations are required.

Table 1 Basic parameters in operating conditions

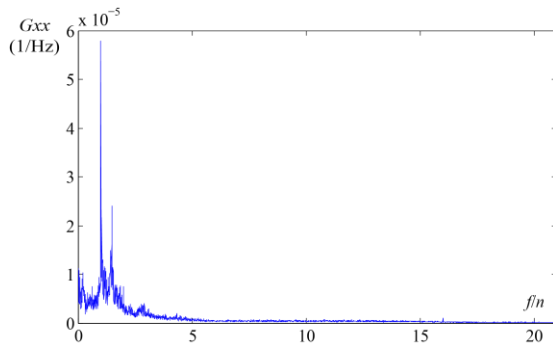|	σ (-)	Q_{ED} (-)	Q/Q_{BEP} (-)	n_{ED} (-)	Turbine rotational frequency (rpm)	Guide vane angle (deg)	E (J/kg)
(i)	0.11	0.055	0.275	0.288	800	5.2	263.64
(ii)	0.11	0.055	0.275	0.317	880	5.1	263.04

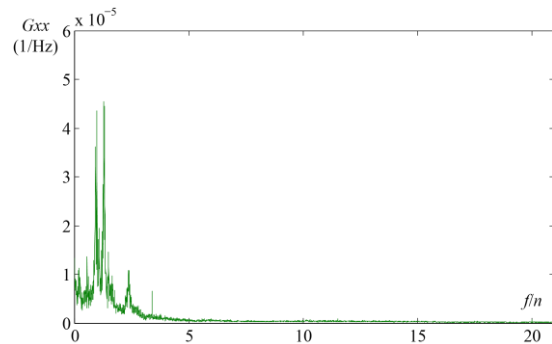(i) $n_{ED} = 0.288$ (100% of nominal n_{ED})   (ii) $n_{ED} = 0.317$ (110% of nominal n_{ED})

Fig. 8 Image of inter blade cavitation vortices at $Q_{ED} = 0.055$ and $\sigma = 0.11$

(i) $n_{ED} = 0.288$ (100% of nominal n_{ED})   (ii) $n_{ED} = 0.317$ (110% of nominal n_{ED})

Fig. 9 Frequency analysis result *Gxx* of the pressure fluctuation in the draft tube cone with the non-dimensional frequency f/n at $Q_{ED} = 0.055$ and $\sigma = 0.11$
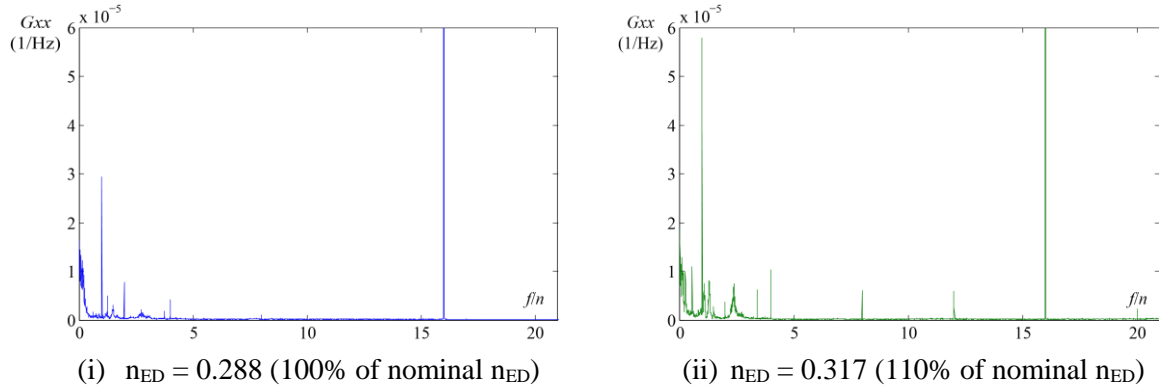
(i) $n_{ED} = 0.288$ (100% of nominal n_{ED})   (ii) $n_{ED} = 0.317$ (110% of nominal n_{ED})

Fig. 10 Frequency analysis result *Gxx* of the pressure fluctuation in the guide vane
with the non-dimensional frequency *f/n* at $Q_{ED} = 0.055$ and $\sigma = 0.11$

5. Conclusion and next steps

In this study, the cavitation phenomena at deep part load condition are investigated especially focusing on the cavitation vortex rope as well as inter-blade cavitation vortices. As a result, the cavitation vortex rope in the cone disappears at about 30% of Q_{BEP}, then inter-blade cavitation vortices are observed at 110% of the nominal n_{ED} around this discharge condition. Although the pressure fluctuations at $n_{ED} = 0.288$ are similar to the ones at $n_{ED} = 0.317$ in the frequency domain for the presented conditions, further investigations are required to obtain a better understanding of the inter-blade cavitation vortices. In the next steps, the authors intend to investigate the pressure fluctuations in the blade channel to survey the influence of the inter-blade cavitation vortices on the runner blades.

Nomenclature

D_{ref}	: Reference diameter of runner	*NPSE*	: Net Positive Suction Energy
E	: Turbine specific energy	Q	: Discharge
Gxx	: One-sided autospectral density	Q_{ED}	: IEC flow rate factor
f	: Frequency	σ	: Cavitation number (Thoma number)
n	: Turbine rotational frequency	Subscription	
n_{ED}	: IEC speed factor	BEP	: Best Efficiency Point

Reference

[1]   Rheingans, W. J. (1940). Power Swings in Hydroelectric Power Plants, Transaction of ASME 62, pp.171-184

[2]   Avellan, F. (2004). Introduction to Cavitation in Hydraulic Machinery, Proc. of the *6th International Conference on Hydraulic Machinery and Hydrodynamics*, Timisoara, Romania

[3]   Jacob, T., Prenat, J., Vullioud, G. and Lopez Araguas, B. (1992). Surging of 140MW francis turbines at high load, analysis and solution, Proc. of the *16th IAHR Symposium on Hydraulic Machinery and Systems*. Sao Paolo, Brazil

[4]   Koutnik, J., Pulpitel, L. (1996). Modeling of the Francis turbine full-load surge, Proc. Of the *Modeling, Testing and Monitoring for Hydro Power Plants*, Lausanne, Switzerland, Session 3, pp.143-154

[5]   Müller, A., Dreyer, M., Andreini, N., Avellan, F. (2013). Draft tube discharge fluctuation during self-sustained pressure surge: Fluorescent particle image velocimetry in two-phase flow, *Experiments in Fluids*, Vol.54, Issue 4, pp.1-11

[6]   Alligné, S., Nicolet, C., Tsujimoto, Y, Avellan, F. (2014). Cavitation Surge Modelling in Francis Turbine Draft tube, *Journal of Hydraulic Research*, Article in press

[7]   Nishi, M., Matsunaga, S., Kubota, T., Senoo, Y. (1982) Flow Regimes in an Elbow-Type Draft Tube, Proc. of the *11th IAHR Symposium on Hydraulic Machinery and System*, Amsterdam, Netherlands, Paper No.38, pp.1–13

[8]   Favrel A., Landry C., Müller A. and Avellan F. (2012). Experimental identification and study of hydraulic resonance test rig with Francis turbine operating at partial load, Proc. of the *26th IAHR Symposium on Hydraulic Machinery and Systems* Beijing, China

[9]   Farhat, M., Natal, S., Avellan, F., Paquet, F. and Couston, M. (2002). Onboard Measurements of pressure and strain Fluctuations in a Model of Low Head Francis Turbine – Part 1: Instruction, Proc. of the *21th IAHR Symposium on Hydraulic Machinery and Systems*, Lausanne, Switzerland

[10]   Lowys, P. Y., Paquet, F., Couston, M., Farhat, M., Natal, S. and Avellan, F. (2002). Onboard Measurements of pressure and strain Fluctuations in a Model of Low Head Francis Turbine – Part 2: Measurements and Preliminary Analysis Results, Proc. of the *21th IAHR Symposium on Hydraulic Machinery and Systems*, Lausanne, Switzerland

[11]   Escaler, X., Egusquiza E., Farhat, M., Avellan, F. and Coussirat, M. (2006). Detection of cavitation in hydraulic turbines, *Journal of Mechanical Systems and Signal Processing*, Vol.20, Issue4, pp.983-1007